Second International Symposium on Marine Propulsors
smp'11, Hamburg, Germany, June 2011

Numerical and Experimental Study of Propeller Ventilation

Anna Maria Kozlowska[1], Katja Wöckner[2], Sverre Steen[1], Thomas Rung[2]
Kourosh Koushan[3], Silas J.B. Spence[3]

[1] Department of Marine Technology, Norwegian University of Science and Technology (NTNU), Trondheim, Norway
[2] Institute of Fluid Dynamics and Ship Technology, Hamburg University of Technology, Hamburg, Germany
[3] MARINTEK, Norwegian Marine Research Technology Institute, Trondheim, Norway

ABSTRACT

The primary objective of the numerical and experimental study of propeller ventilation is to obtain knowledge about the forces acting on thrusters in heavy seas. To address this problem, a joint European project, PropSeas, has been established. One aspect of the project's activities is to investigate the forces acting on the propeller during ventilation events, and how the occurrence of ventilation depends on different operational parameters, like submergence and propeller loading. This paper is largely based on the comparison between the model test conducted by MARINTEK and calculations performed by TUHH. The comparison contains two main tasks: a comparison between blade forces and moments during non-ventilating and ventilating phases; as well as a comparison between flow visualization using high-speed video (experiments) and CFD simulation. The comparisons aim at indentifying the degree of correlation, and reasons for deviations are discussed. It is found that while the agreement for non-ventilating conditions is very good, CFD generally overpredicts the propeller forces in ventilating conditions. Also, the variation of thrust on a single blade over a revolution is larger in CFD than in the model tests. It is believed that this is caused by the inability to resolve thin ventilating vortices in the RANS Volume of Fluid type CFD calculations.

Keywords

Propeller ventilation, thrust loss, vortex ventilation, torque loss.

SYMBOLS INDEX

h/R	[–]	Propeller submergence ratio
J	[–]	Advance ratio
K_T	[–]	Thrust coefficient
K_{T0}	[–]	Nominal thrust coefficient
K_{TBLADE}	[–]	Blade thrust coefficient
K_Q	[–]	Torque coefficient
K_{Q0}	[–]	Nominal torque coefficient
K_{QBLADE}	[–]	Blade torque coefficient
FS		Free surface
TUHH		Hamburg University of Technology

1 INTRODUCTION

The intermittent ventilation of conventional propellers is a challenge for ships operating in heavy seas, and especially when operating at low forward speeds and/or high propeller loadings, something that is typical for most offshore vessels. Ventilation leads to a sudden large loss of propeller thrust and torque, which might lead to propeller racing and possibly damage dynamic loads, as well as noise and vibrations. The effect of ventilation on average thrust and torque of propellers operating in waves is discussed by several researchers; see, e.g., Shiba (1953), Fleisher (1973), Faltinsen (1981, 1983), Minsaas (1975, 1981, 1983), Olofsson (1996), Koushan (2006, 2007, 2009) and Kozlowska (2009). Shiba (1953) discussed the influence of different propeller design parameters, e.g., expanded area ratio, contour of blade, radial variation of pitch, skewback, effect of rudder, turbulence of original flow, as well as scale effects on ventilation. Ventilation effects with respect to vessel operation in addition to added resistance in waves and reduction of propulsive efficiency can be found in Faltinsen (1981, 1983) and Minsaas (1975, 1981, 1983). Olofsson (1996) studied the force and flow characteristics of surface piercing propellers. Koushan (2006, 2007) performed extensive model tests on an azimuth thruster with 6 DoF measurements of forces on one of the four blades on an azimuthing thruster, as reported in four papers (Koushan 2006 I, II, III, 2007). Kozlowska (2009) focused on ventilation inception mechanisms, classification of types of ventilation, thrust loss related to each type of ventilation, and a simple calculation method for predicting thrust loss.

Experimental investigation of the effect of waves and ventilation on thruster loadings has been performed by

Koushan (2009). The comparison between numerical and experimental study of propeller ventilation can be found in the Califano (2009). The aim of this paper is to document the degree of correlation between calculations and model tests.

The comparison contains two main tasks: comparison between blade forces (thrust) and moments (torque) during non-ventilating and ventilating phases, as well as a comparison between flow visualization using high-speed video (experiments) and CFD simulations.

1.1 CFD Calculations

The CFD calculations presented in this article are performed by TUHH and are based on the in-house code FreSCo$^+$ (Schmode 2007). The viscous CFD-method FreSCo$^+$ is a spin-off of FreSCo, a joint development of TUHH, the Hamburg Ship Model Basin (HSVA) and the Dutch Maritime Research Institute (MARIN). The method is a RANS code based on a finite volume discretisation of the computational domain. For modeling the free surface a Volume of Fluid technique (Muzaferij 1999) is used. Thus, an equation for the volume fraction ($0 \leq c \leq 1$) is solved to distinguish the water phase ($c=0$) from air ($c=1$). Additionally, specific interface sharpening techniques are also available to capture violent deformations of the interface without an unphysical mixture of water and air.

For the investigations presented below, the propeller is modeled in a cylindrical domain, which rotates with the number of revolutions of the propeller.

1.2 Experiment

The experiments were conducted in the Large Towing Tank at MARINTEK. The four-bladed right-handed propeller was mounted on the open water test rig. A novel blade dynamometer capable of measuring 5 degrees of freedom (the centrifugal component was not measured) was used during these experiments. The use of high-speed video cameras (one under and one above water) gives a visual understanding of ventilation phenomena.

1.2.1 Data Filtering

In order to capture the dynamics, a high sampling frequency of 1200 Hz was used during these experiments. The power spectrum of blade thrust for the raw data from experiments is plotted in Figure 1 below where the peaks due to propeller loads and due to noise can be noticed. A low-pass filter with a cutting frequency of 160Hz was applied for the comparison. Figure 2 shows that the dominant frequency is the propeller frequency both for non- ventilating and fully ventilating cases.

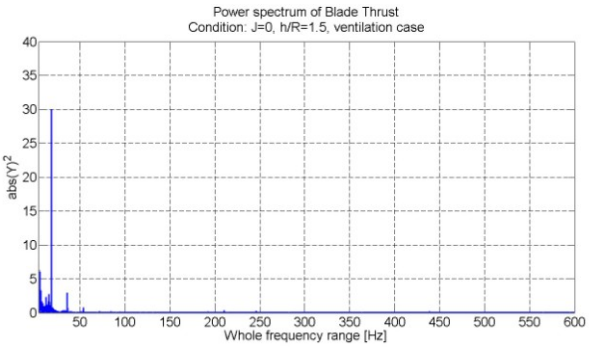

Figure 1: Whole frequency range, ventilation phase

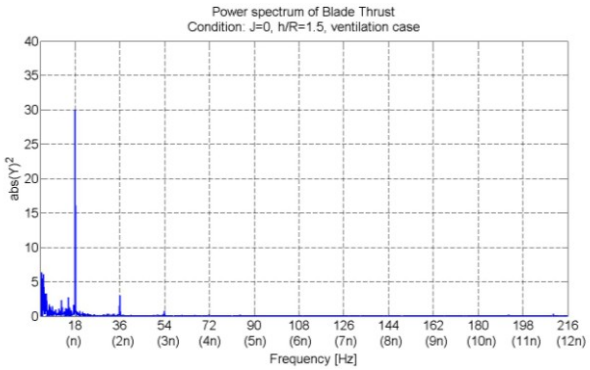

Figure 2: Propeller and blade frequency range, ventilation phase

1.2.2 Co-ordinate System

In order to have better comparison between calculations (TUHH) and experiments (MARINTEK) the same system of co-ordinates were used in this article.

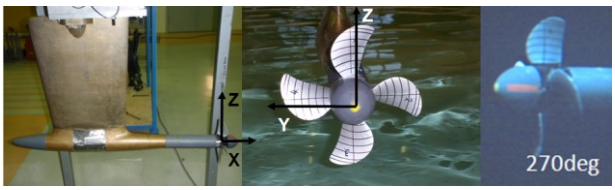

Figure 3: Employed co-ordinate system

In this co-ordinate system, x is the axis in propeller shaft direction. Thus FX_B is the blade thrust and MX_B is the blade torque. The measurement blade was Number 1 and was marked by a red line on the propeller hub cap.

2 COMPARISON MATRIX

Experimental tests were conducted for four submergence ratios h/R=2.5, 1.5, 1 (when the blade tip is touching the free surface (FS)) and 0 (when half of the propeller is out of water). For all four submergences the carriage speed was varied in order to obtain the following advance ratios (J=0, 0.15, 0.3, 0.45, 0.6, 0.75, 0.9, 1.05, 1.2). Propeller revolution was constant and equal to 18 Hz. Calculations were performed for two propeller submergences h/R=2.5, 1.5 and six propeller advance ratios (J=0.001, 0.15, 0.3, 0.6, 0.9 and1.2)

3 THRUST AND TORQUE COEFFICIENT – DEFINITION

Thrust and torque coefficients are defined as follows:

$$K_T = \frac{T_t}{\rho n^2 D^4}, K_{T0} = \frac{T_n}{\rho n^2 D^4} \quad (1)$$

$$K_Q = \frac{Q_t}{\rho n^2 D^5}, K_{Q0} = \frac{Q_n}{\rho n^2 D^5} \quad (2)$$

K_T/K_{T0}=1 means no thrust loss and K_T/K_{T0}=0 means total thrust loss due to ventilation and out of water effects.

4 DEEP WATER RESULTS

Figure 4 shows the thrust and torque coefficients of the propeller blade in non-ventilating, deep water conditions (h/R=2.5). Experimental data from the towing tank tests with blade dynamometer are compared with CFD calculations and open water test with normal propeller dynamometer. The comparison is satisfactory although experiments and CFD calculations overpredicted the thrust and torque compared with the open water test with propeller dynamometer. The agreement between CFD calculations (TUHH) and experiments is quite good.

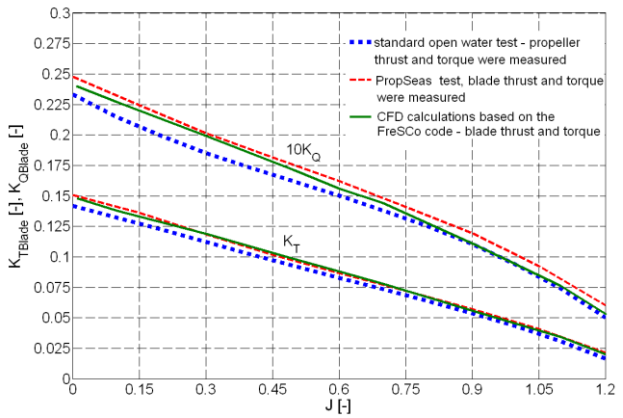

Figure 4: Deep water thrust and torque coefficients for a single blade.

5 COMPARISON BETWEEN CALCULATIONS AND EXPERIMENTS, h/R=1.5

5.1 J=0

5.1.1 Comparison between Calculations and Experiments Blade Thrust and Torque

Figure 5 shows the thrust and torque coefficients divided by nominal thrust and torque coefficient as a function of blade position for a sequence of propeller revolutions. It can be observed from the figure that the variation in thrust and torque between revolutions is less for calculations than for the experimental results. However, the number of revolutions simulated (18) is much less than in the experiments (1620). Thus, it might be that the current CFD calculations only capture one of several possible "flow modes". During measurements the thrust loss is quite constant during revolution and depends on the duration of the experiments. In the CFD, blade thrust has a strong variation with position, with large thrust loss around top position and small thrust loss around bottom position. This difference might be explained by the fact that in the calculation the blade loses contact with the air-supplying vortex.

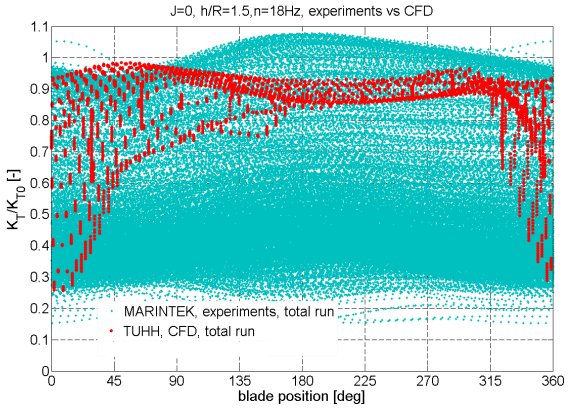

Figure 5: Thrust ratio during each revolution

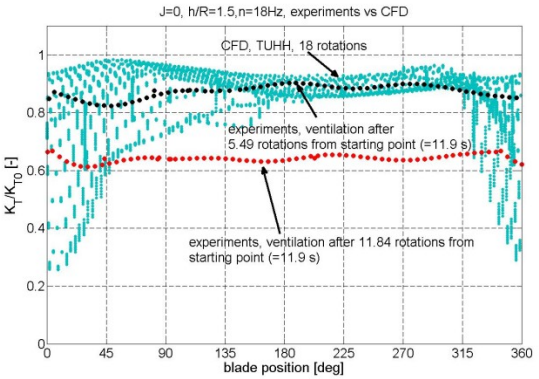

Figure 6: Torque ratio during each revolution

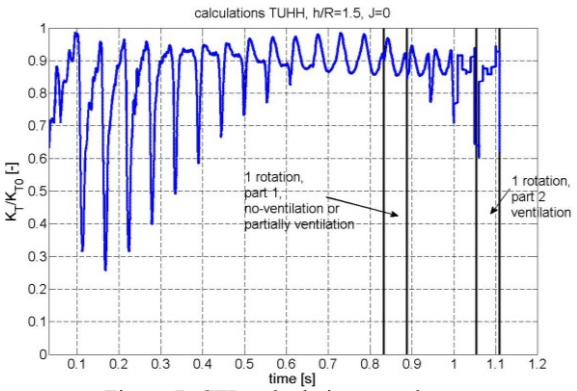

Figure 7: CFD calculations, total run

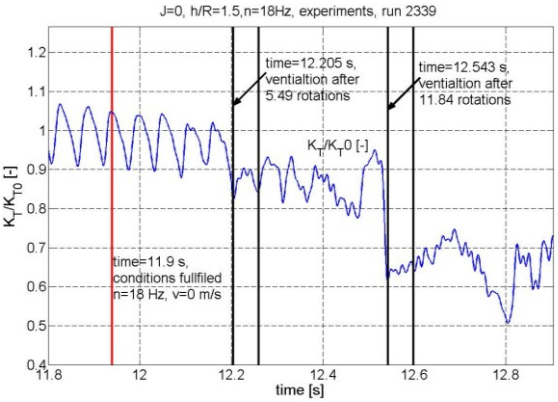

Figure 8: One of the first thrust drops, experiments

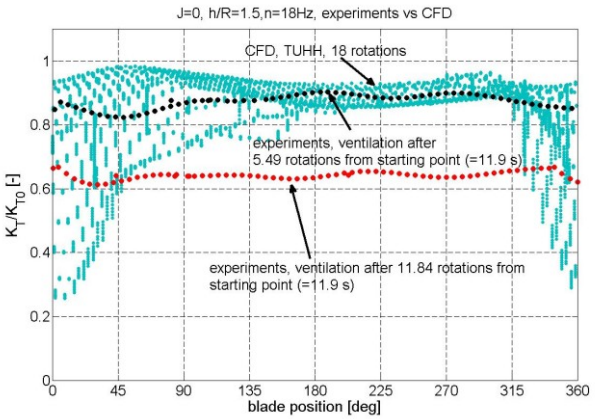

Figure 9: Comparison between one of the first thrust drops and CFD calculations

Figure 7 shows that the total time of CFD simulation was about 1.1 s, which correspond to 18 propeller rotations. Figure 8 shows that during the experiments, the first thrust drop occurred after 5.5 rotations from the starting point and another bigger drop occurs after 11.84 rotations. Thus, it can be compared with the CFD simulation since 18 propeller rotations were computed in the CFD simulation. Figure 9 presents the comparison between one of the first thrust drops during the experiments and the CFD calculations.

Note that the influence of the specific initial conditions is still somewhat unclear. While the propeller starts with the nominal number of revolutions and the flow field is initialized with the inflow velocity in the CFD calculations, the carriage is started after starting the propeller.

5.1.2 COMPARISON BETWEEN CALCULATIONS AND EXPERIMENTS FLOW VISUALISATION

Figure 10 shows a comparison between thrust coefficient for the CFD simulations and the experiments during non-ventilating and partially ventilating phases. Photo 1 and Photo 2 correspond with a sequence of photos from the experiments; Part 1 and Part 2 correspond with screenshots of simulation performed by TUHH.

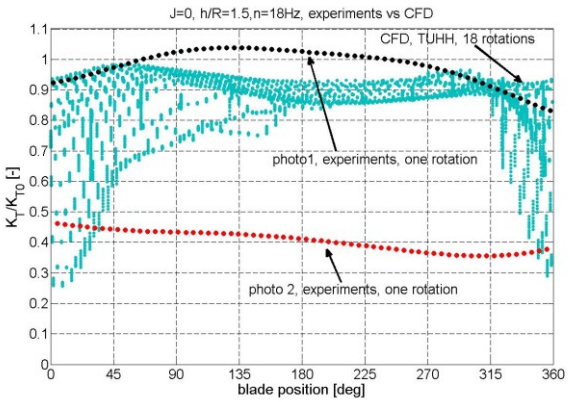

Figure 10: Thrust ratio for photo cases chosen for comparison with CFD calculation

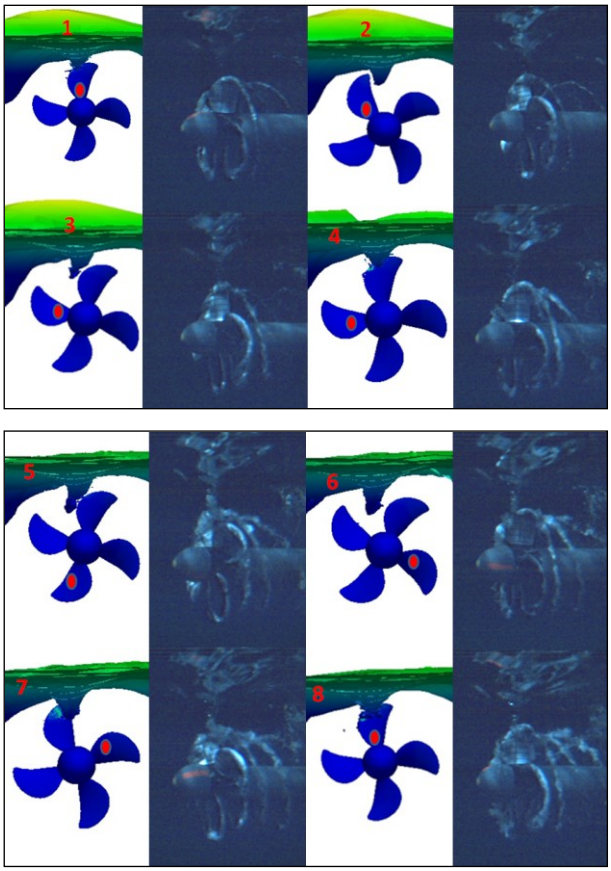

Figure 11: J=0, no or partially ventilating regime, one rotation, Experiments: Photo 1, CFD: time (0.833s:0.888s),

Figure 11 shows that the mechanism for ventilation inception is similar for the calculation and for the experiments. Also, comparison between thrust ratios is quite good. Due to propeller rotation, ventilation starts by forming an air-filled vortex from FS. The vortex mainly appears in the blade position between 315-45 deg.

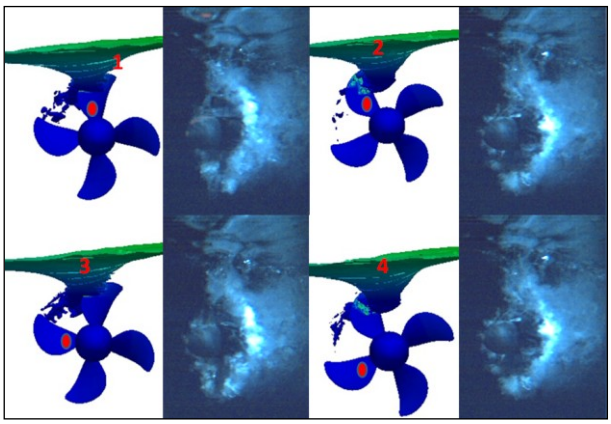

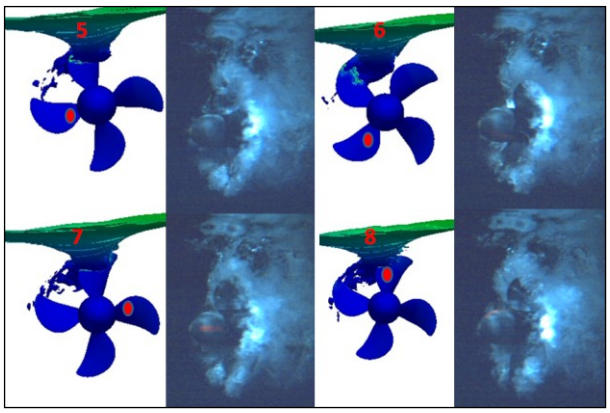

Figure 12: J=0, fully ventilating regime, one rotation, Experiments: Photo 2, CFD: time (1.0545s:1.11s)

Figure 12 show that the propeller ventilated more during the experiments. The tip vortex sucked down the air from FS and transported it in the direction of the propeller rotation; most of the air was transported downstream. In the experiments, we observe an air cloud covering the entire blade, which indicates a fully ventilating propeller. This is believed to be caused by a stronger connection between blade and vortex in the experiment than in the corresponding CFD calculation. During CFD simulation, the blade loses the connection with a vortex after passing 90 deg and we cannot observe a fully ventilating case. This might be due to problems with resolving a thin ventilating vortex in CFD. Also, problems representing air bubbles in the CFD might be a reason for the large difference in visual appearance.

5.2 J=0.15

5.2.1 Comparison between Calculations and Experiments Blade Thrust and Torque

Figure 13 shows that prediction of thrust loss is more repeatable between revolutions for the calculations than for the experiments. On the other hand, the variations during a revolution are larger for the CFD results than for the experiments. During simulation, we can observe a similar thrust loss for every propeller revolution. The biggest thrust loss is when the blade is close to the FS (between 315 and 90 deg). For the propeller blade position between 90 and 315, the thrust is built up again and achieves values close to nominal thrust. During measurements, we observe different thrust losses depending on the time in the experiments. The different thrust losses correspond to different ventilation extents. It is clear from the experiments that in this condition, the propeller can be both fully and partly ventilating, and that it changes between the different ventilating conditions without an apparent reason. When the propeller starts ventilating, the thrust loss is bigger than for the simulation. Also, in ventilating condition, the experiments typically show almost no variation in thrust during a single revolution.

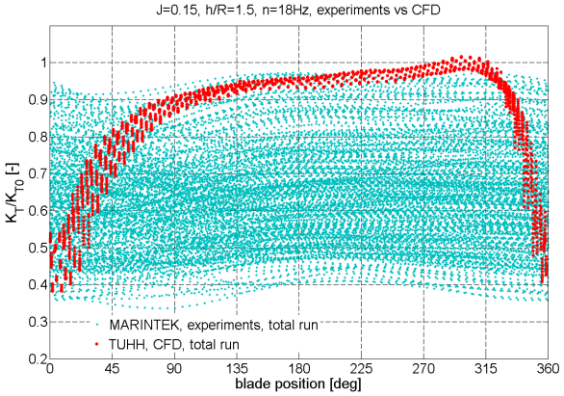

Figure 13: Thrust ratio during each revolution

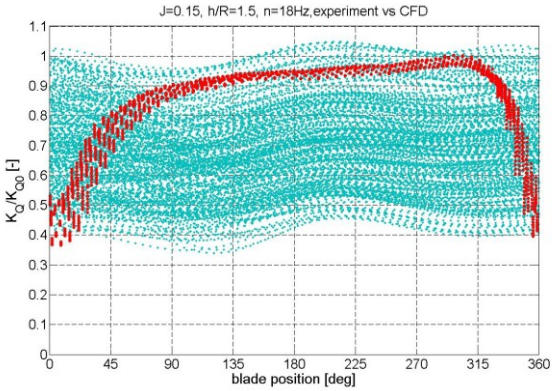

Figure 14: Torque ratio during each revolution

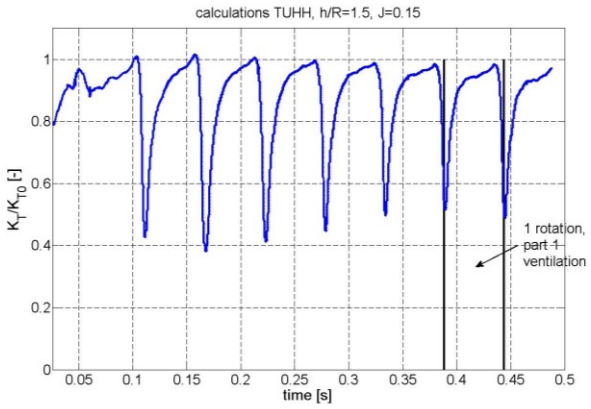

Figure 15: CFD calculations, total run

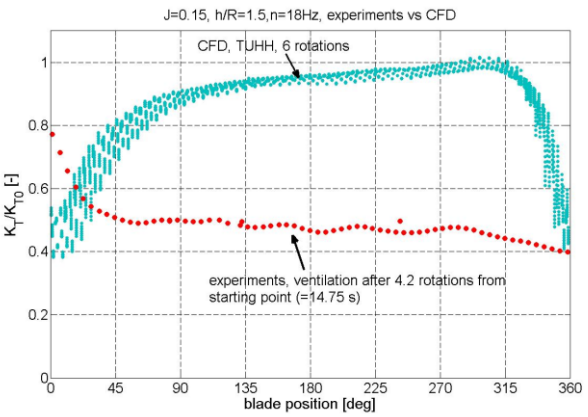

Figure 16: One of the first thrust drops, experiments

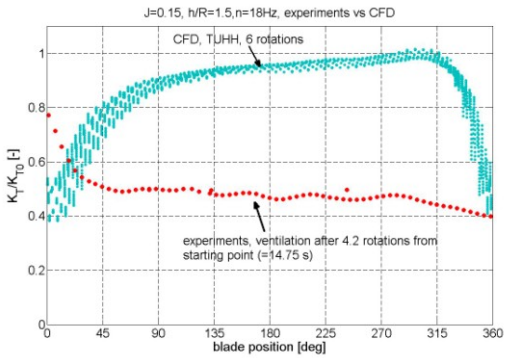

Figure 17: Comparison between one of the first thrust drops and CFD calculations

5.2.2 Comparison between Calculations and Experiments Flow Visualisation

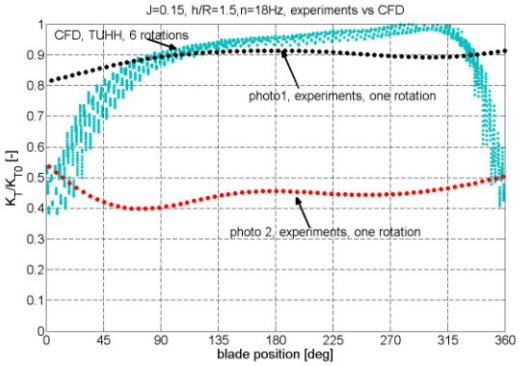

Figure 18: Thrust ratio for photo cases chosen for comparison with CFD calculations

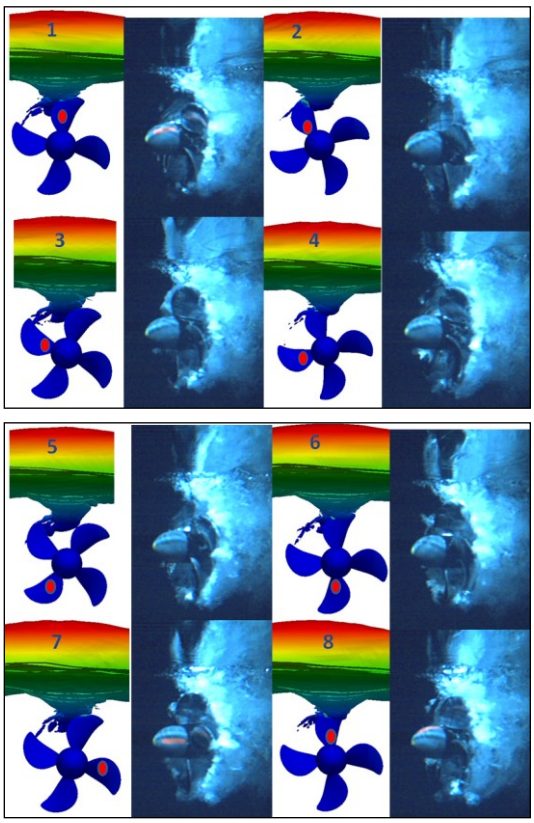

Figure 19: Experiments: Photo 2, CFD: time (0.3885s:0.444s), one rotation.

It is worth mentioning that it is difficult to predict thrust losses based on the flow visualization from the experiments. Figure 20 shows a comparison between two different propeller rotations and the same blade position. The photos look very similar: a similar blade area is covered with air, but the blade thrust ratio is different for these two cases.

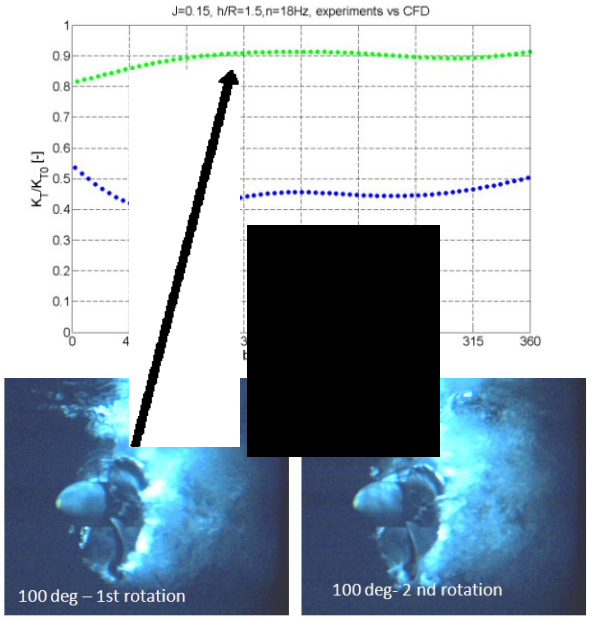

Figure 20: Comparison between two different propeller rotations and the same blade position.

5.3 J=0.3

5.3.1 Comparison between Calculations and Experiments Blade Thrust and Torque

Figure 21 shows that the thrust loss is bigger in the experiment. The main reason for this phenomenon is the time difference between the simulations and the experiments. During the experiments (J=0.15, n=18Hz, h/R=1.5) 20s of measurements were recorded, which correspond to 360 propeller rotations. In order to compare these results with the calculations, we should have the same number of propeller revolutions. For the calculations, only 6 propeller rotations were computed. The same phenomenon is observed for torque.

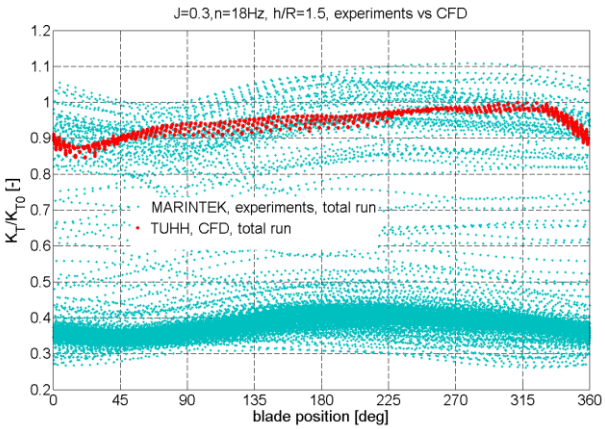

Figure 21: Thrust ratio during each revolution

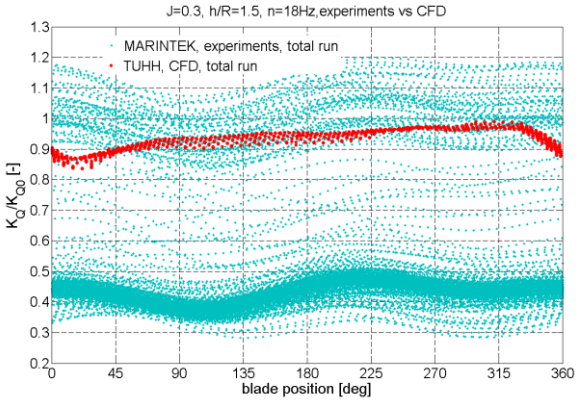

Figure 22: Torque ratio during each revolution

5.3.2 Comparison between Calculations and Experiments Flow Visualisation

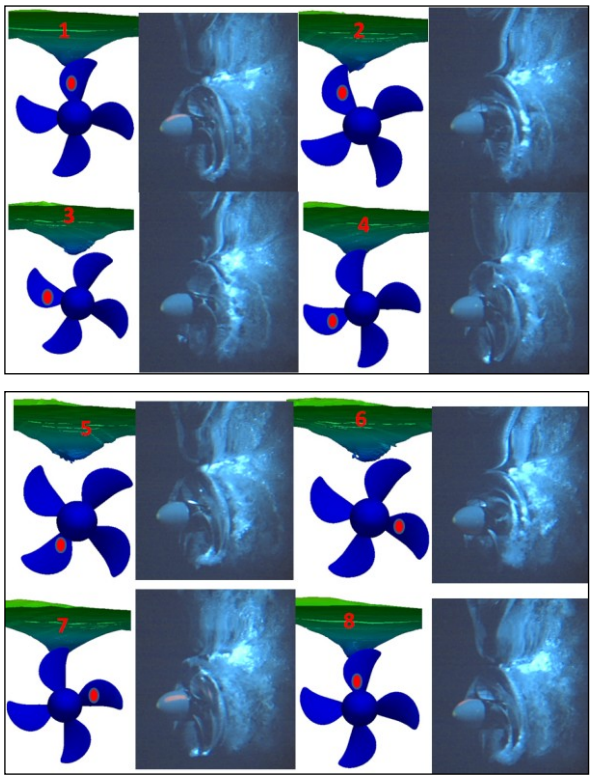

Figure 23: J=0.3, Experiments and CFD, fully or partially ventilating regime ventilating regime, one rotation

5.4 J=0.6

5.4.1 Comparison between Calculations and Experiments Blade Thrust and Torque

Figures 24 and 25 show good agreement between the calculations and the experiments. We observe no thrust and torque loss during this case. This is because for high advance numbers (J=0.6) the flow suppress the vortex and ventilation does not start in this case.

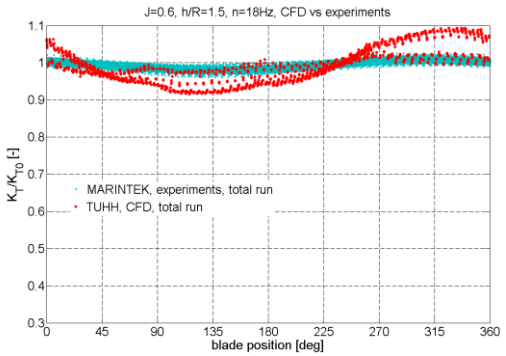

Figure 24: Thrust ratio during each revolution

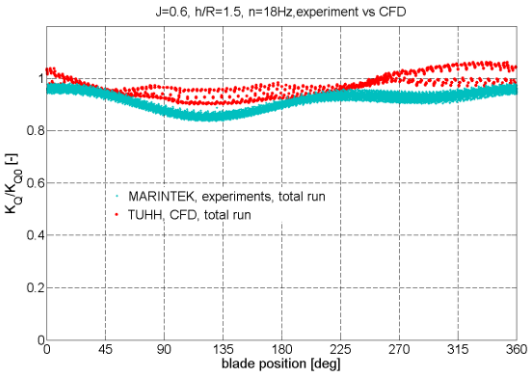

Figure 25: Torque ratio during each revolution

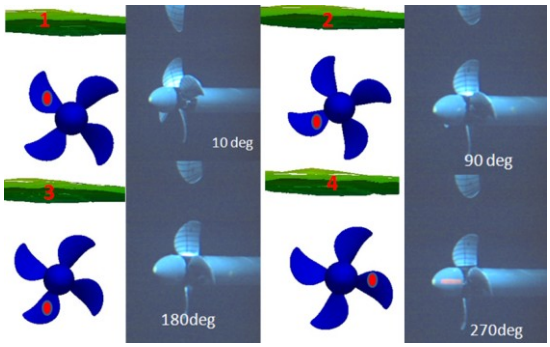

Figure 26: J=0.6, Experiments and CFD, non ventilating regime, one rotation

6 CONCLUSIONS

Based on the comparisons presented in this article the following conclusions have been drawn:

1) Thrust ratio for non-ventilating regime shows good correlation between the experiments and the calculations. The same good agreement is observed for the torque ratio.

2) Flow visualization recorded by high-speed camera and simulation shows that the propeller ventilates more during the experiments than predicted by CFD. Ventilation starts by forming tip vortex, which sucks down the air from the free surface and transports it in the direction of the propeller rotation. During the experiments, the vortex is connected much longer to the blade than for the calculations. This might be due to problems with

resolving a thin ventilating vortex in CFD. Also, problems representing air bubbles in the CFD might be a reason for the large difference in visual appearance.

3) In order to have a better comparison between CFD and experiments, the simulation time and time duration of experiments should be more similar. The excessive amount of CPU time required makes it very difficult to perform computations for the same total number of revolutions as in the experiment. Table 1 compares the time until the first ventilation event for experiments, and compares it to the number of revolutions simulated in CFD. Although the minimum requirement – first ventilation event (see Table 1 below) - was fulfilled for all presented cases, we see that the simulated time is very short compared to the time-scale of the ventilation, and as a result, important phenomena might be missing from the simulation results due to the short simulated time.

Experiments		CFD
	First ventilation event	Number of rev. during whole simulation
J=0	1st- After 5.5 rotations 2nd- After 11.84 rotations	20
J=0.15	After 4.2 rotations	8
J=0.3	After 6.2 rotations	8
J=0.6, 0.9, 1.05,1.2	No ventilation	8
Table1. Minimum requirement for ventilation based on experimental data		

4) For the lowest advance ratios (J=0, 0.15, 0.3), there is a marked difference between the experiments and the calculations with respect to how blade thrust varies with blade position. In the CFD, blade thrust has a strong variation with position, with large thrust loss around top position and small thrust loss around bottom position; while in the experiments the thrust loss is quite constant during a revolution. This difference might be explained by the fact that in the calculation the blade soon loses contact with the air-supplying vortex, while in the experiments it looks like the blade is continuously supplied with air from the surface.

ACKNOWLEDGEMENT

This work was carried out as a part of the Research European Project PropSeas. MARINTEK, Rolls-Royce, NTNU, TUHH, University of Duisburg-Essen, Farstad, GL and Develogic are research partners in the project.

REFERENCES

Califano, A. & Steen, S. (2009). 'Analysis of different propeller ventilation mechanisms by means of RANS simulation'. SMP09, Trondheim, Norway.

Faltinsen, O., Minsaas, K. J., Liapias, N. & Skjørdal. (1981). 'Prediction of resistance and propulsion of a ship in a seaway'. The Shipbuilding Research Association, Japan.

Fleischer, K. P. (1973). 'Untersuchungen über das Zusammenwirken von Schiff und Propeller teilgetauchten Propellern'. Forschungszentrum des Deutschen Schiffbaus Bericht **130**(73).

Koushan, K. (2006 I). 'Dynamics of ventilated propeller blade loading on thrusters'.

Koushan, K. (2006 II). 'Dynamics of Ventilated Propeller Blade Loading on Thrusters Due to Forced Sinusoidal Heave Motion'. Rome, Italy.

Koushan, K. (2006 III). 'Dynamics of Propeller Blade and Duct Loadings on Ventilated Ducted Thrusters Operating at Zero Speed'. 3-5 October 2006.

Koushan, K. (2007). 'Dynamics of Propeller Blade and Duct Loadings on Ventilated Ducted Thrusters Due to Forced Periodic Heave Motion'. Proceedings of International Conference on Violent Flows, Fukoka, Japan.

Koushan, K. 'Dynamics of Propeller Blade and Duct Loadings on Ventilated Thrusters in Dynamic Positioning Mode'. Proceedings of Dynamic Positioning Conference, Houston, TX, United States.

Koushan, K., Spence, S. J. B. & Hamstad, T. (2009). 'Experimental Investigation of the Effect of Waves and Ventilation on Thrusters Loadings'. SMP09, Trondheim, Norway.

Kozlowska, A. M., Steen, S. & Koushan, K. (2009). 'Classification of Different Type of Propeller Ventilation and Ventilation Inception Mechanisms'. SMP09, Trondheim, Norway.

Minsaas, K., Wermter, R. & Hansen, A. G. (1975). 'Scale Effects on Propulsion Factors'. Towing Tank Conferences, Proceedings Volume 3.

Minsaas, K., Faltinsen, O. & Person, B. (1983). 'On the importance of added resistance, propeller immersion and propeller ventilation for large ships in seaway.' Proceedings of International Symposium on Practical Design of Ships and other Floating Structures PRADS, Tokyo & Seoul.

Muzaferij, S. & Peric, M. (1999). 'Computation of free-surface flows using interface-tracking and interface capturing methods'. Nonlinear Water Wave Interaction, pp. 59-100.

Shiba, H. (1953). 'Air Drawing of Marine Propellers'. Transportation Technical Research Institute, Report **9**, Japan, Aug. 1953.

Schmode, D. & Rung, T. (2007). 'Rans-code verification using method of manufactured solution'. 10th Numerical Towing Tank Symposium, Hamburg, Germany.

Olofsson, N. (1996). Force and Flow Characteristic of a Partially Submerged Propeller. PhD Thesis, Department of Naval Architecture and Ocean Engineering Division of Hydrodynamics, Goteborg, Sweden.